Human CD4$^+$CD25^{low} Adaptive T Regulatory Cells Suppress Delayed-Type Hypersensitivity during Transplant Tolerance[1]

Qingyong Xu,[2]* Junglim Lee,[2]*† Ewa Jankowska-Gan,* Jackie Schultz,* Drew A. Roennburg,* Lynn D. Haynes,* Satoshi Kusaka,* Hans W. Sollinger,* Stuart J. Knechtle,* Anne M. VanBuskirk,‡ Jose R. Torrealba,§ and William J. Burlingham[3]*§

Adaptive T regulatory (T_R) cells mediate the suppression of donor-specific, delayed-type hypersensitivity (DTH) in tolerant organ transplant recipients. We hypothesized that cells belonging to the CD4$^+$CD25$^+$ T cell subset but distinct from natural T_R cells may fulfill this role. To test this hypothesis, PBMC and biopsy samples from two tolerant kidney transplant recipients (K1 and K2) were analyzed. When transferred with recipient APC into a SCID mouse footpad, CD4$^+$ T cells were hyporesponsive in DTH to donor type HLA-B Ags and derivative allopeptides. However, anti-human TGF–β1 Ab revealed a response to immunodominant allopeptides in both patients, suggesting that CD4$^+$ T effector (T_E) cells coexisted with suppressive, TGF–β1-producing CD4$^+$ T_R cells. During in vitro culture, allopeptide stimulation induced both IFN-γ-producing and surface TGF–β1$^+$ T cells. The relative strength of the latter response in patient K1 was inversely correlated with the level of systemic anti-donor DTH, which varied over a 6-year interval. Allopeptide-induced surface TGF–β1 expression was found primarily in Forkhead box P3 (FoxP3)–negative CD4$^+$CD25^{low} T cells, which could adoptively transfer suppression of donor-specific DTH. Biopsy samples contained numerous surface TGF-β1$^+$ mononuclear cells that costained for CD4 and, less frequently CD25, but were negative for FoxP3. The CD4$^+$TGF-β1$^+$ T cells were localized primarily to the tubulointerstitium, whereas TGF-β1$^-$FoxP3$^+$CD25$^+$ cells were found mainly in lymphoid aggregates. Thus, adaptive T_R cells suppressing T_E cell responses to donor allopeptides in two tolerant patients appear to be functionally and phenotypically distinct from CD4$^+$CD25^{high}FoxP3$^+$ T cells. ***The Journal of Immunology,*** **2007, 178: 3983–3995.**

Homeostatic equilibrium between Ag-specific T regulatory (T_R)[4] cells and T effector (T_E) cells has been proposed to account for certain paradoxical features of the adaptive immune system. For example, the preservation of immunocompetent T memory cells in chronic parasite or viral infection (1, 2) has been attributed to a T_R-dominant T_R-T_E homeostasis, as has the protection of malignant melanoma from tumor Ag-specific rejection (3), the maintenance of transplantation tolerance (4–6), the control of inflammatory bowel disease (7), the TGF-β1-dependent reversal of recent onset diabetes by anti-CD3-antibody in the NOD mouse (8), and the beneficial effects of anti-CD3 mAb therapy in human insulin-dependent diabetes mellitus clinical trials (9). Most but not all of the above studies have implicated CD4$^+$ CD25$^+$ T_R cells in the mechanism of specific tolerance. For this reason there has been considerable debate over how to distinguish Forkhead box P3 (FoxP3)-positive "natural" T_R cells (10, 11) from adaptive T_R cells (for a review see Ref. 12). Although it seems clear that most human natural T_R cells are CD4$^+$CD25^{high} and that they nonspecifically suppress the proliferation of CD4$^+$CD25$^-$ T cells in a contact-dependent manner (13), they can also induce the latter to become adaptive CD4$^+$ T_R cells producing TGF-β1 and/or IL10 in response to specific Ag challenge (14). Whether or not such adaptive T_R cells also acquire a FoxP3$^+$CD25^{high} phenotype in the process is still controversial (15, 16).

Under certain circumstances, the transplantation of organs and tissue results in tolerance rather than rejection. This type of acquired tolerance takes various forms from unstable to metastable to stable, reflecting the extent of its resistance to specific antigenic challenge in an immunogenic context (17). Classical skin transplantation tolerance in mice is donor specific, i.e., there is no acceptance of a third party allograft (18). Yet Graca et al. (19) found that transfer of CD4$^+$CD25$^+$ T_R cells from a tolerant mouse blocked third party as well as donor-specific allograft rejection, a "paradoxical" result. No attempt was made to separate adaptive from natural T_R cells, leaving open the possibility that natural T_R cells with nonspecific immunosuppressive properties may have overwhelmed the Ag-specific effects of adaptive T_R cells present in the CD4$^+$CD25$^+$ T cell pool.

Studies of Ag-specific regulation in CD8$^+$ T cells (20, 21) have been more successful in clearly distinguishing the adaptive immune component in acquired tolerance. In both mouse and human minor histocompatibility Ag-specific tolerance, Ag-specific CD8 T_R cells may have lower avidity for cognate Ag/MHC than CD8

*Department of Surgery, University of Wisconsin, Madison, WI 53792; †Department of Microbiology, College of Medicine, Konyang University, Nonsan, South Korea; ‡Department of Surgery and Comprehensive Cancer Center, Ohio State University, Columbus, OH 43210; and §Department of Pathology, University of Wisconsin and Veterans Affairs Hospital, Madison, WI 53792

Received for publication May 18, 2006. Accepted for publication January 5, 2007.

The costs of publication of this article were defrayed in part by the payment of page charges. This article must therefore be hereby marked *advertisement* in accordance with 18 U.S.C. Section 1734 solely to indicate this fact.

[1] This work was supported in part by National Institutes of Health Grants R21-AI49900-01, R01-AI/HL 48624-01, and K02-AI01452, Immune Tolerance Network Grant 1814-8094 (to W.J.B.), a grant from the University of Wisconsin Medical Foundation (to J.L.), University of Wisconsin Graduate School Grant 135G144 (to Q.X.), and National Institutes of Health Grants U19-AI43900 (to S.J.K.) and R29-AI40909 and P30-CA16058 (to A.M.V.).

[2] Q.X. and J.L. contributed equally to this work.

[3] Address correspondence and reprint requests to Dr. William J. Burlingham, G4/702 Clinical Science Center, 600 Highland Avenue, Madison, WI 53792. E-mail address: burlingham@surgery.wisc.edu

[4] Abbreviations used in this paper: T_R, T regulatory; DTH, delayed-type hypersensitivity; FoxP3, Forkhead box P3; LKP, leukapheresis; T_E, T effector; TT, tetanus toxoid.

Copyright © 2007 by The American Association of Immunologists, Inc. 0022-1767/07/$2.00

T_E cells (20, 22), yet they can also suppress T_E cell-driven delayed-type hypersensitivity (DTH) responses by means of TGF-β1 production (20, 23, 24). These features allow clear distinctions to be made between adaptive T_E and T_R cells.

Based on previous work in rhesus macaques (4) and humans (20, 25), we have proposed a model of tolerance to an organ allograft that is based on a dynamic equilibrium between alloantigen-specific T_R cells and T_E cells (26). Adoptive transfer studies of selected T cell populations combined with transplantation may be used to test such a mechanism in animal models, breaking tolerance as needed and then rescuing with infusions of T_R cells. However, in human studies such an approach is not feasible. One way to test such a model in the clinical transplant setting would be to take advantage of the metastable nature of tolerance itself in the course of a long-term follow-up. For example, by leukapheresis (LKP) and cryopreservation of PBMC at different times posttransplant one may compare putative T_E and T_R cell fractions from time points of anti-donor hyporesponsiveness when the equilibrium between donor-specific T_E and T_R cells favors the T_R and contrast this with the same cell fractions obtained during a period of high responsiveness to a donor when such an equilibrium has broken down. The adoptive transfer can then be done using a surrogate in vivo assay system such as the trans-vivo DTH test (20, 27).

We hypothesized that human adaptive CD4$^+$ T_R cells, which recognize cognate allopeptide/self-MHC complexes via the indirect allorecognition pathway, are functionally and phenotypically distinct from FoxP3$^+$ CD4$^+$ T_R cells. To test this hypothesis, we used PBMC from two patients with HLA-mismatched kidney transplants and stable renal function >2 years after discontinuing all immunosuppression. We were also able to monitor one of these patients over a 6-year period after initial enrollment in our study. By flow cytometry, flow sorting, and functional assays, we found that the CD4$^+$CD25^{low} subset of PBMC in both patients contained surface TGF-β1-inducible, allopeptide-specific T_R cells, whereas PBMC from an HLA-B-sensitized patient, K3, lacked such cells. These T_R cells were able to suppress anti-donor DTH reactions while CD4$^+$CD25^{high} cells did not. Furthermore, immunohistochemical analyses of biopsy samples indicated that CD4$^+$TGF-β1$^+$ T_R cells in the accepted allograft occupy a niche anatomically distinct from that of FoxP3$^+$CD25$^+$ T_R cells during allograft tolerance.

Materials and Methods

HLA typing and source of PBMC

PBMC were obtained by sterile venipuncture or LKP, further purified by Ficoll-Hypaque density gradient separation, and cryopreserved until use. All blood and LKP samples were obtained by informed consent subject to Institutional Review Board (University of Wisconsin, Madison, WI) approval. HLA-A and -B typing was performed by standard complement-dependent cytotoxicity techniques; for patient K1 and donor HLA-B serologic typing was confirmed by high resolution sequence-specific primer PCR, whereas HLA-DR/DQ typing was performed by low resolution sequence-specific PCR.

Ags and peptide preparation

The donor Ag was either a cell sonicate of donor PBMC, a cell sonicate of the 721.221 lymphoblastoid cell line singly transferred with donor-type HLA (B8, B7), or a soluble recombinant HLA-B*1501 (B62). Donor Ags were prepared and used with methods described previously (25, 28, 29). Recall Ags such as tetanus toxoid (TT; Lederle Laboratories) and EBV (Viral Antigens) were used as described (25, 28). Four 18-mer oligopeptides were synthesized and purified (>94% pure) at the Biotechnology Facility at the University of Wisconsin (Madison, WI).

Flow cytometric analysis and cell sorting

All anti-human mAbs and secondary reagents for flow cytometric analysis, if not specifically noted, were obtained from BD Pharmingen. Flow cytometry was performed on a FACSCalibur or SLR II (BD Biosciences), analyzed with CellQuest (BD Biosciences), or FlowJo (Tree Star) software. CD4$^+$ and CD8$^+$ T cells (purity >98%) were sorted from whole PBMC by FACSVantage (BD Biosciences) with CD4-FITC/CD8-PE mAbs (Beckman Coulter). Different fractions of CD4$^+$ CD25$^{high/low/-}$ cells (purity >98%) were flow sorted from whole PBMC or MACS-enriched CD4$^+$ T cells. For certain experiments CD4$^+$ or CD8$^+$ T cells were also MACS-depleted using anti-CD4/CD8 beads (Miltenyi Biotec); depletion was typically >99% of starting CD4 or CD8 T cells.

Cell culture and surface TGF-β1 staining

PBMC (8×10^5/well) or CD4$^+$CD25$^{high/low/-}$ cells ($1\sim2 \times 10^5$ cells/well) plus irradiated CD4$^-$ cells (<0.5% CD4$^+$ T cells used as APC, 10^6/well) were cultured with peptides or anti-CD3 (clone OKT3; 10 μg/ml) in 100 μl/well IMDM (Cambrex) with 2% Serum Replacement 3 (Sigma-Aldrich), L-glutamine, 1 mM sodium pyruvate, and 2% penicillin-streptomycin for 40 h at 37°C with 5% CO_2 and stained with biotinylated chicken anti-human TGF-β1 (R&D Systems) or biotinylated chicken IgY control (Jackson ImmunoResearch Laboratories) and secondary reagents. The specific induction of surface TGF-β1$^+$ cell was determined by subtracting the background percentage of the TGF-β1$^+$ value for self-peptide p37-TE-stimulated cells (where TE refers to threonine and glutamic acid). Rat anti-human FoxP3-FITC (clone PCH101; eBioscience) and rat IgG2a (BD Pharmingen) were used with the protocol described by the vender.

Trans-vivo DTH assay

The trans-vivo DTH assay was used as described (25). Ags (1 μg/ml) were injected along with 9×10^6 whole PBMC (or CD4/CD8-depleted PBMC) or $3–4 \times 10^6$ separated T lymphocytes plus 8×10^5 Percoll-purified APC into the footpads of female CB17 SCID mice (Harlan Breeders). In some experiments, RAG$^{(-/-)}$/TGF–β1$^{+/+}$ single-knockout mice or RAG2$^{(-/-)}$/TGF-β1$^{(-/-)}$ double-knockout mice bred from a line of RAG-2$^{(-/-)}$/TGF-β1$^{+/-}$ parental mice on a C57BL/6 × 129 hybrid background and provided by Dr. T. Doetschman (University of Cincinnati College of Medicine, Cincinnati, OH) were used. Animals were housed and treated in according with American Association of Laboratory Animal Care and National Institutes of Health guidelines. In linked suppression assays, recall Ags (such as TT and EBV) were coinjected with PBMC alone or with donor Ag to detect donor-specific T_R cells. To reveal suppressed DTH responses, rabbit anti-human TGF-β (pan-specific) or control normal rabbit IgG (R&D Systems) were used for cytokine neutralization experiments if not specifically noted otherwise; anti-human CTLA-4 blocking mAb/control mouse IgG1 (Ab Solutions) was also used to reverse suppression. For a DTH assay with purified T cells, APC (purity of >90% CD14$^+$) were enriched from PBMC by discontinuous Percoll density gradient centrifugation as described previously (30). Residual T and B cells were depleted by incubating the 1.062 density fraction with mouse anti-human CD2 and mouse anti-human CD20 (Beckman Coulter), followed by goat anti-mouse-IgG magnetic beads (Dynal) separation.

DTH results are reported as mean ± SD of 2–10 independent experiments measuring changes in footpad thickness in units of 10^{-4} inches 24 h postinjection after subtraction of background swelling due to the injection of PBMC plus PBS alone.

Anti-HLA Ab detection

Anti-HLA Abs were detected in human serum by indirect immunofluorescence using fluorescence-labeled beads coated with single HLA class I or class II Ags (Luminex single HLA Ag test kit, One Lambda). Specific immunofluorescence values for a given batch of beads vary; therefore, results are reported as a ratio of specific Ag-to-background fluorescence for each clinical specimen tested.

ELISPOT assay

An IFN-γ ELISPOT assay was performed as described elsewhere (31). Briefly, 96-well polyvinylidene difluoride plates (Whatman) were coated with anti-human IFN-γ capture Ab (5 μg/ml; BD Pharmingen). Human PBMC (3×10^5/well) were plated with different peptides (300 μg/ BD Pharmingen). After incubation at 37°C with 5% CO_2 for 48 h, a secondary Ab (2 μg/ml; BD Pharmingen) was added and then developed with ELISPOT Blue Color Module (R&D Systems) and read with the AID ELISPOT reader system ELR02 (Cell Technology).

Table I. *HLA-A,-B,-DR typing and description of patients and donors*

Patients[a]	HLA typing (HLA-B Ags selected for detailed study are indicated in boldface type)	
	Donor	Recipient
K1[b]	A1, 2; B44, **62**[c]; DR4, 6[d]	A1, 2; B37, 60; DR4, 6[e]
K2[f]	A2, 26; **B8, 57**; DR2, 7	A2, –; B14, 22; DR1, 6[g]
K3[h]	A2, 3; B7, **62**; DR13, 15	A2, 3; B7, 8; DR4, 15
L1[i]	A25, 28; B47, **62**; DR4, 7	A2, 29; B7, 44; DR15, –[j]

[a] Underlined designations indicate tolerant transplant recipients.
[b] Kidney transplant from a deceased donor in 1993 for reflux nephropathy. Off insulin 1995; clinical course described as patient DS elsewhere (25) and in Fig. 3.
[c] Serologically defined HLA-B Ag. By molecular typing this was designated as B*1501.
[d] HLA-DR molecular type DRB1*4011, *1301.
[e] HLA-DR molecular type DRB1*0407, *1301.
[f] Kidney transplant from a deceased donor in 1986 for chronic glomerulonephritis; ceased insulin in 2003 due to renal carcinoma in native kidney that was removed in 2004. Current serum creatinine is 1.1 mg/dl.
[g] HLA-DR molecular type DRB1*0102, *1302.
[h] Kidney transplant from haploidentical sibling as part of a tolerance induction trial, currently on rapamycin monotherapy. Current serum creatinine is 1.3 mg/dl.
[i] Liver recipient in 1986 currently on triple therapy with prednisone, mycophenolate mofetil, and tacrolimus; described as patient BK previously (28).
[j] DRB1*1501, —.

H&E histopathology and TGF-β FoxP3 immunohistochemistry

Biopsies were graded according to the Banff criteria (32) of renal allograft pathology on H&E staining of paraffin-embedded tissue. Paraffin-embedded or frozen sections of biopsy were immunolabeled using mAbs against TGF-β1 (clone TB21) as described (4). For paraffin sections only the heat-induced epitope retrieval method (33) with an EDTA buffer (pH 8.0) (Borg; Biocare Medical) was used. Fluorescent immunolabeling was performed as described (4) with anti-CD4, anti-CD-8, and anti-CD25 at a 1/40 dilution. Sections were visualized with a fluorescent microscope (Olympus B X51) and images analyzed with image software (Diagnostic Instruments, version 3.2.1).

For immunoperoxidase dual labeling studies, FoxP3 (rabbit anti-human polyclonal; Abcam Ab 10563) and CD25 (mouse anti-human monoclonal; Vector VP-C340) as well as TB21 Abs were used on paraffin-embedded tissue after EDTA heat-induced epitope retrieval of Ag. The primary Ab to TGF-β1 or CD25 (1/40 dilution) was incubated for 1 h at room temperature, detected with Mach 2 (Biocare Medical) and color developed with VIP chromogen (purple; Vector Laboratories). Tissue was fixed with 10% formalin and then permeabilized with 0.5% Triton. The second primary Ab to FoxP3 (1/400 dilution) was incubated for 1 h at room temperature, detected with Mach 3 (Biocare Medical), and color developed with diaminobenzidine (brown).

Statistical analysis

Statistical analysis was performed using a randomization test if not specifically noted otherwise. The randomization test based on *t* statistics is much more stringent than the standard *t* test; it is used when evaluating reproducibility of results within experiments using samples drawn from a single patient.

Results

DTH responses to donor HLA-B Ag are CD4 mediated and inhibited by TGF-β1

The HLA-A,-B, and -DR Ags of donors and recipients are shown in Table I. Both of the kidney transplant patients, K1 and K2, were functionally tolerant, i.e., off all immunosuppression for >2 years while retaining excellent kidney function. Patient K1 received a graft from a well-matched HLA-DR/DQ but HLA-B44 and B62 (B*1501)-mismatched deceased donor in 1993. Patient K2 received a graft from a deceased donor in 1986 that was mismatched for 5/6 HLA-A, -B, and -DR Ags, including HLA-B8 and HLA-B57. Patient K3, who developed anti-B*1501-specific HLA Ab in the first year posttransplant, is included as a nontolerant control. A conventionally immunosuppressed recipient of a liver transplant from a fully HLA-mismatched deceased donor (29), patient L1, was included in the study to compare allopeptide specificity of the indirect pathway CD4 T_R cell response to the same HLA-B Ag in a different host MHC class II context.

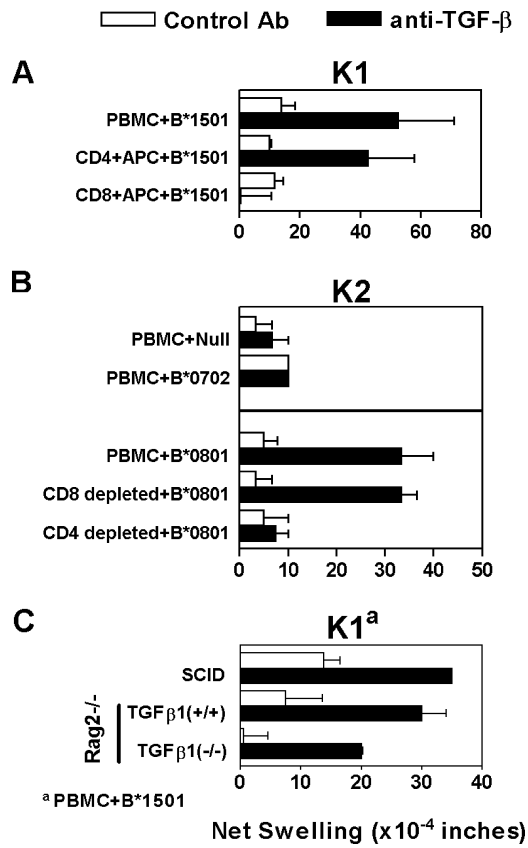


FIGURE 1. Donor HLA-B Ag-specific regulation in two tolerant transplant recipients. PBMC obtained at 5.8 years posttransplant from patient K1 (*A*) or at 18 years posttransplant from patient K2 (*B*) were tested. *A*, $CD4^+$ or $CD8^+$ T cells were positively selected, mixed with APC, and challenged with soluble HLA-B*1501. *B*, CD8- or CD4-depleted PBMC were mixed with sonicates of a HLA-class I "null" 721.221 B lymphoblastoid cell line or 721.221 cells expressing transgenes encoding HLA-B*0702 or HLA-B*0801. *C*, PBMC from patient K1 was coninjected with soluble HLA-B*1501 Ag into the footpad of SCID, $RAG2^{-/-}TGF\text{-}\beta1^{+/+}$, or $RAG2^{-/-}TGF\text{-}\beta1^{-/-}$ mice for a DTH assay. Trans-vivo DTH responses were tested in the presence of control rabbit IgG (*A* and *B*, □) or IgY (*C*, □) or of rabbit anti-TGF-β1 Ab (*A* and *B*, ■) or chicken anti-human TGF-β1 Ab (*C*, ■). Data shown are the mean ± SD of DTH responses measured in units of 10^{-4} inches net footpad swelling (n = 2–4 experiments).

To characterize the indirect pathway of allorecognition of HLA-B Ags, we injected purified soluble HLA proteins or cell lysates containing soluble HLA together with PBMC into the footpads of SCID mice. The PBMC of patient K1 responded weakly to a HLA-B*1501 soluble Ag in the presence of isotope control IgG but showed a strong DTH response when TGF-β1-specific Ab was present (Fig. 1*A*). Separated CD4 T cells plus APC reproduced this response pattern, while separated CD8 T cells failed to respond under either condition.

A slightly different approach yielded a similar result in patient K2. Patient K2 was EBV sero-negative and did not respond in DTH to the EBV Ag (data not shown). We could therefore use cell sonicates of the B lymphoblastoid cell line 721.221, a HLA class I "null" mutant cell line, and sublines transfected with particular HLA-B genes to probe the memory T cell response of K2 to

Table II. *HLA-B peptide sequences*

HLA-B Ag	Peptide	Amino Acid Sequences
B*1501	p106 (p106–123) self	NH_2-DGRLLRGH**D**Q**S**AYDGKDY-COOH
B*1501	p149 (p149–166) self	NH_2-AAREA**E**QW**R**AYLEG**L**CVE-COOH
B*1501; B*5701	p37-MA (p37–54)[a] self	NH_2-DSDAASPR**MA**PRAPWIEQ-COOH
	p37-TE (p37–54) allo	NH_2-DSDAASPR**TE**PRAPWIEQ-COOH
B*0801	p61-F (p61–77)[b] self	NH_2-DRNTQI**F**KTNTQTDRES-COOH
	p61-C (p61–77) allo	NH_2-DRNTQI**C**KTNTQTDRES-COOH

[a] For the peptide defined by the region from aa 37 to aa 54 we designated the donor allopeptide p37-MA where "MA" refers to the polymorphic residues methionine and alanine at positions 44 and 45 (in boldface type), whereas the corresponding "self" peptide p37-TE has threonine and glutamic acid. The MA polymorphism is found predominantly in only two common Caucasian HLA-B Ags, HLA-B*1501 and HLA-B57, a mismatched HLA-B Ag for patient K2.

[b] The polymorphic phenylalanine (F) amino acid is present at position 67 (in boldface type) in all HLA-B8 family members, whereas the cysteine (C) amino acid (boldface type) is present in the HLA-B14 of patient K2.

HLA-B Ags without complication from responses to EBV proteins expressed in the cell lysates. TGF-β1 neutralization restored a positive DTH response in whole PBMC to HLA-B*0801 but not to a third party Ag HLA-B*0702 or to HLA class I-negative, 721.221 cell sonicates. The restoration of response to HLA-B*0801 in the presence of an anti-TGF-β1 Ab was abrogated by the depletion of CD4$^+$ but not by depletion of CD8$^+$ T cells (Fig. 1*B*). Thus, in each case the T_E cells that responded to donor-type soluble HLA Ags when TGF-β1 was neutralized were CD4$^+$. The anti-IL-10 Ab, which blocks T_R and restores T_E cell function in some transplant recipients (25), was also tested but did not reveal a significant anti-donor DTH response in these two subjects (data not shown).

A reversal of DTH hyporesponsiveness to HLA-B*1501 in the PBMC of patient K1 by an anti-TGF-β1-specific Ab was also seen in the footpad of a RAG-2/TGF-β1 double-knockout mouse, indicating that murine TGF-β1 was not required for the suppression of B*1501-specific T_E function in K1 PBMC (Fig. 1*C*).

Allopeptide specificity of donor HLA-B-reactive CD4$^+$ T_R and T_E cells

To further define the specificity of the DTH response of CD4$^+$ T cells to donor-type HLA-B Ags, four allopeptides and two self-peptides were synthesized based on a comparison of donor and recipient HLA-B amino acid sequences and the identification of polymorphic residues that differed between the two (Table II). We compared responses to HLA- B*1501- or HLA-B*0801-derived allopeptides in the presence of a control rabbit IgG or an anti-TGF-β Ab. PBMC from patient K1 contained T_E capable of mediating a strong DTH response to the peptide p37-MA (where MA refers to methionine and alanine) but not to p106 or p149. This response required recipient APC (data not shown). The level of DTH response to p37-MA when TGF-β1 was neutralized was equivalent to the response to intact soluble HLA-B*1501 Ag, indicating that the p37 peptide contained the immunodominant epitope (compare Fig. 2*A* with Fig. 1*A*). In the conventionally immunosuppressed liver transplant recipient L1, also mismatched for HLA-B*1501 with her donor, a positive DTH response was revealed by TGF-β1 neutralization when PBMC were challenged with soluble HLA-B*1501, p106 (weakly), and p149, but there was no response to p37-MA (Fig. 2*A*, *right panel*). These results indicate that the CD4 T cells in patients K1 and L1 recognized different immunodominant epitopes, consistent with the difference in their HLA-DR alleles (Table I). In patient K2, TGF-β neutralization revealed a significant ($p < 0.01$ vs control antibody) DTH response to the HLA-B*0801 allopeptide p61-F, and, surprisingly,

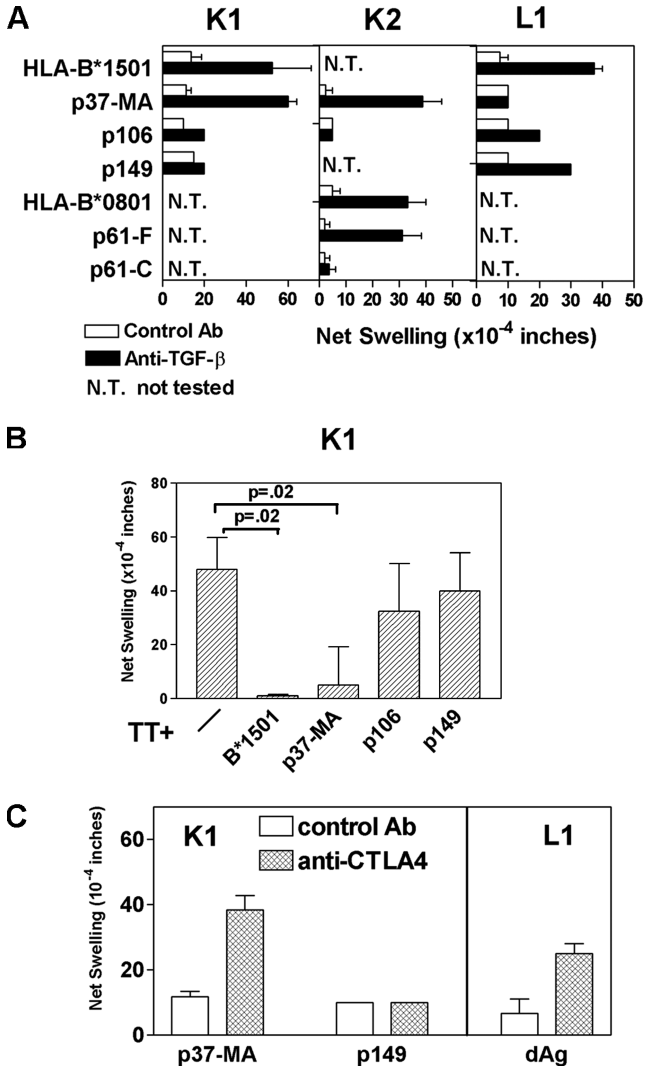


FIGURE 2. DTH regulation is allopeptide specific. *A*, Whole PBMC obtained 5.8 (patient K1), 18 (patient K2), or 3.5 years (patient L1) post-transplant were tested for DTH response to HLA-B*1501 or various HLA-B-derived peptides in the presence of control (□) or anti- TGF-β1 Ab (■). *B*, PBMC of patient K1 plus HLA-B*1501 Ag or allopeptides were tested for linked suppression of recall DTH response to TT. Control was TT alone plus PBMC. *C*, PBMC (from patients K1/LKP1 or L1) plus peptides or a sonicate of donor cells (dAg) were tested with control (□) or anti-CTLA-4 Ab (crosshatched bars) in a DTH assay. Data shown are the mean ± SD (n = 2–7 experiments).

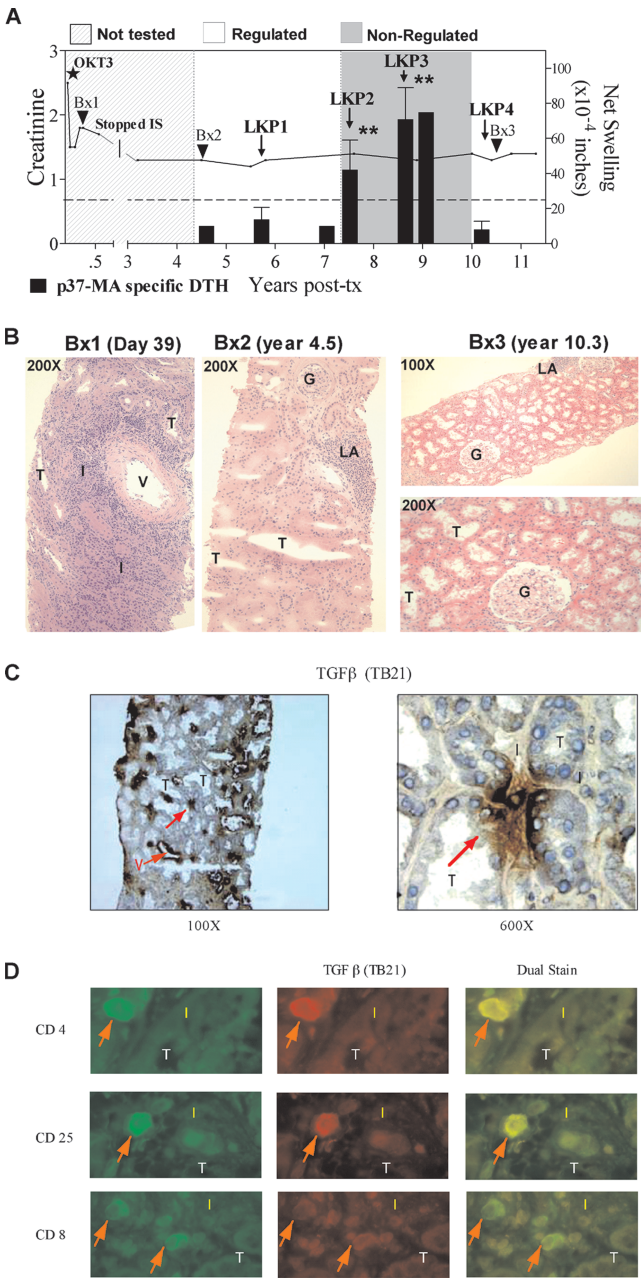


FIGURE 3. Clinical course of patient K1 in relation to DTH responses in PBMC and TGF-$\beta1^+$ cells in the graft. *A*, Posttransplant serum creatinine level (solid line), allograft biopsy (Bx) time points, and anti-donor allopeptide p37-MA-specific DTH responses (■) are shown. DTH analysis was done between year 4.5 and year 10.5 posttransplant (post-tx). LKPs were obtained at four time points (LKP1–4). A period of high anti-donor DTH response (**, $p < 0.001$ LKP2 and 3 vs LKP1 and 4; "nonregulated") is highlighted in gray. DTH data for LKP are the mean ± SD ($n = 6$–10 experiments). *B*, Histology (H&E staining; ×100 to ×200 original magnification) of transplant biopsies from day 39 (*left panel*), year 4.5 (*center panel*), year 10.3 (*right panel*, two views) posttransplantation. T, Tubule; I, interstitium; V, vessel; G, glomerulus; LA, lymphoid aggregate. *C*, Immunostaining profile of TGF-$\beta1^+$ interstitial cells infiltrating the accepted renal allograft at year 4.5. *Left panel*, Immunoperoxidase staining of TGF-$\beta1$ in biopsy frozen section using mAb TB21; a positively stained blood vessel (V) and a zone of positive staining adjacent to a tubule are highlighted by red arrows (×100 original magnification). *Right panel*, Higher power view of the latter showing a central positive cell surrounded by positively stained interstitium (I) and renal tubular basement membrane. *D*, Dual immunofluorescence study of TGF-$\beta1$ expression by T cell subsets in paraffin-embedded section (×600 original magnification). *Left column*, Green staining identifies $CD4^+$, $CD25^+$, or $CD8^+$ cells, the positions of which are indicated by arrows; *center column*, red staining identifies TGF-$\beta1^+$ cells in same field; *right column*, overlay showing dual-staining cells in yellow.

Table III. *Quantitative analysis of TGF$\beta1^+$ cells infiltrating kidney allografts of K1 and K2 number of cells per 10 tubules (mean ± SD)*[a]

Cell Phenotype	K1 (year 10.5)	K2 (year 18)
$TB21^+$	5.0 ± 1.0	3.5 ± 0.5
$CD4^+$	1.0 ± 0.2	8.5 ± 1.0
$CD4^+TB21^+$	0.4 ± 0.1	3.5 ± 0.5
$CD8^+$	0.22 ± 0.05	6.0 ± 1.0
$CD8^+TB21^+$	ND[b]	ND[b]
$CD25^+$	ND[b]	1.0 ± 0.2
$CD25^+TB21^+$	ND[b]	0.2 ± 0.05

[a] At least 20 high power fields were counted for each determination; see Ref. 4 for details.
[b] Not detected.

to p37-MA present in donor-type HLA-B*5701. There was no response to peptides p61-C or p106 (Fig. 2*A*, *middle panel*).

To determine whether $CD4^+$ T_R cells followed the same epitope specificity pattern as the $CD4^+$ T_E cells revealed by TGF-$\beta1$ neutralization, we used linked suppression of the recall DTH response to TT as a readout of T_R function (25). Only the p37-MA peptide was able to reproduce the strong bystander DTH inhibition effect seen with intact HLA-B*1501 in patient K1 (Fig. 2*B*), suggesting that the epitope, which was immunodominant for the $CD4^+$ T_R cells, is the same one recognized by the T_E cells.

The function of the allopeptide-specific T_R cells in these patients was clearly dependent upon TGF-$\beta1$. To see whether CTLA-4 was also required, we used a blocking Ab specific for human CTLA-4. This Ab revealed a strong p37-MA-specific DTH response in patient K1 PBMC (Fig. 2*C*). We found a similar effect of a CTLA-4 blockade, revealing DTH to the donor Ag in the PBMC of patient L1 (Fig. 2*C*, *right panel*).

Time course of metastable tolerance in patient K1

Although some tolerant patients may maintain donor-specific hyporesponsiveness throughout their posttransplant course, in others anti-donor DTH and CTL activity may resurface after a long period of quiescence (34, 35). This "metastable" feature of allotolerance, which in some cases may result in transplant rejection, creates an opportunity in longitudinal studies for comparisons to be made by the adoptive transfer of putative regulatory cells. An example of metastable alloreactivity after transplant is illustrated in Fig. 3. K1 received two doses of anti-CD3 (clone OKT3) mAb at the time of transplant followed by maintenance immunosuppression with azathioprine, prednisone, and cyclosporine. Despite these measures, an episode of biopsy-proven acute cellular rejection occurred on day 39 (Fig. 3*A*), which was reversed by additional OKT3 therapy. Unfortunately, no PBMC were available from this time period for immunoassay analysis. K1 discontinued all immunosuppressive drugs of his own volition at year 1.5. When tested for kidney function at year 3, his serum creatinine was still in the normal range (1.3–1.4 mg/dl) and has remained so up to the present. K1 was monitored regularly for anti-donor DTH responses in peripheral blood beginning at year 4.5. DTH responses to p37-MA were consistently low over a 3-year period. However, a strongly positive DTH response to p37-MA (Fig. 3*A*) and HLA-B*1501 (data not shown) was detected in PBMC beginning at year 7.5. A 2.5 year "nonregulated" period followed, characterized by strong anti-donor DTH responses (Fig. 3*A*, gray area). A third LKP

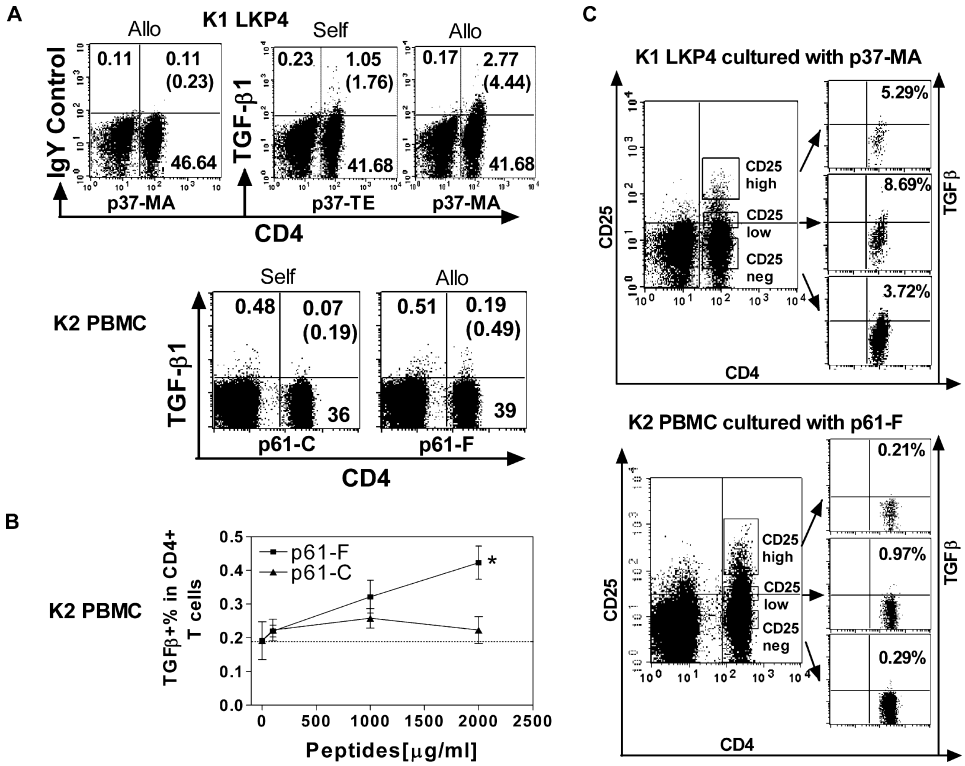


FIGURE 4. Surface TGF-β1expression is a marker for allopeptide-induced CD4$^+$ T_R cells. *A*, *Top panels*, Flow histograms of PBMC from patient K1 (LKP4) that had been cultured for 40 h with control self-peptide p37-TE or allopeptide p37-MA. Anti-CD4 and IgY control (*top left*) or chicken anti-TGF-β1 Ab dual staining cells as a percentage of gated lymphocytes are indicated in the *upper right quadrant*. Numbers in parentheses are the percentages of CD4 T cells. *Bottom panels*, Same analysis using K2 PBMC cultured with control self-peptide p61-C or allopeptide p61-F. *B*, Percentages of peptide-specific TGF-β1$^+$ T_R cells induced in CD4$^+$ T cells from PBMC of patient K2 with different peptide concentrations. Data shown are the mean $\pm$ SD (n = 4–7 experiments). $*$, $p < 0.01$ vs p61-C. *C*, Flow histograms of PBMC from patients K1 (*top panel*) and K2 (*bottom panel*) cultured with allopeptide and stained for CD4, CD25, and surface TGF-β1. Different fractions of CD4$^+$ T cells were gated for high, low, and negative CD25 expression as shown, and the percentages of TGF-β1$^+$ cells in each gate were determined. Shown is a representative experiment of seven.

(LKP3) was obtained at year 8.6. After year 10, the DTH response to p37-MA returned to baseline at which time a fourth LKP was performed (LKP4). The key point for mechanistic studies is that samples with low DTH response to donor were captured in LKP 1 and 4, allowing comparison with samples of high response in LKP 2 and 3.

Transplant biopsy samples from KI showed several interesting histologic features. On day 39 classic features of acute rejection, including tubulitis, vasculitis, and extensive mononuclear cell infiltration, were observed. Biopsies taken at year 4.5 and 10.3 post-transplant, however, showed histopathologic features of tolerance previously described in rhesus monkey and human kidney transplants (4, 36, 37). These features included lymphoid aggregates, scattered interstitial mononuclear cell infiltrates, and an absence of tubulitis, allograft vasculopathy, interstitial fibrosis, or tubular atrophy (Fig. 3*B*, *middle* and *right panels*).

Previous immunohistochemical analysis of tolerance in the rhesus monkey renal transplant model revealed interstitial mononuclear infiltrates containing CD4$^+$ T cells that produce a latent complex form of TGF-β1 detected by the mAb TB21 (4). As shown in Fig. 3*C*, immunoperoxidase staining of frozen sections of the year 4.5 biopsy revealed abundant TB21$^+$ immunostaining in the renal parenchyma, including both vascular endothelium-associated and mononuclear cell-bound TGF-β1. No immunostaining of mononuclear cells was observed using the mAb 1D11 specific for active TGF-β1 (data not shown). As shown in detail in a higher power view of a single TGF-β1$^+$ interstitial cell ($\times$600 original magnification; red arrow), the outer rim of the cell was intensely stained, as was the surrounding matrix and the basolateral aspect of the surrounding tubules (Fig. 3*C*, *right panel*).

To determine the surface phenotype of the TGF-β1$^+$ cells in the year 4.5 biopsy sample, we used dual immunofluorescence labeling. As shown in Fig. 3*D*, the green fluorescence signal for CD4 (*top row of panels*, $\times$600 original magnification), but not that for CD8 (*lower row of panels*), colocalized with a strong TGF-β1 red fluorescence signal (*center column of panels*), producing a bright yellow color on overlay (*top right panel*). The peritubular TGF-β1$^+$ infiltrates included some cells that costained with anti-CD25 Ab (Fig. 3*D*, *middle row of panels*), although these were less frequent than the ones that costained with anti-CD4. A quantitative analysis of cells in the tubulointerstitium was performed on the year 10.3 biopsy of patient KI as well as the year 18 biopsy of patient K2. We used an immunoperoxidase labeling method on paraffin-embedded tissue reported previously (4) to score the graft-infiltrating cells in a blinded fashion and tabulated the results. The analysis confirmed the presence of CD4/TGF-β1 dual-stained T cells, the absence of CD8/TGF-β1 dual-stained cells, and the relative paucity or absence of CD25/TGF-β1 dual-stained T cells (Table III). Importantly, approximately one-third of the CD4$^+$ T cells were costained for TGF-β1, while CD25$^+$ cells were either undetectable (K1) or of low frequency (K2) in the peritubular areas of both transplants.

Adaptive CD4$^+$ T_R cells express surface TGF-β1 after in vitro challenge

The cell surface-associated expression of TGF-β1 by CD4$^+$ T cells in the biopsies of accepted kidney allografts suggested a way to directly visualize donor allopeptide-specific CD4$^+$ T_R cells in peripheral blood. PBMC from K1 (LKP4) and K2 were cultured with peptides for 40 h and tested for surface TGF-β1 expression by

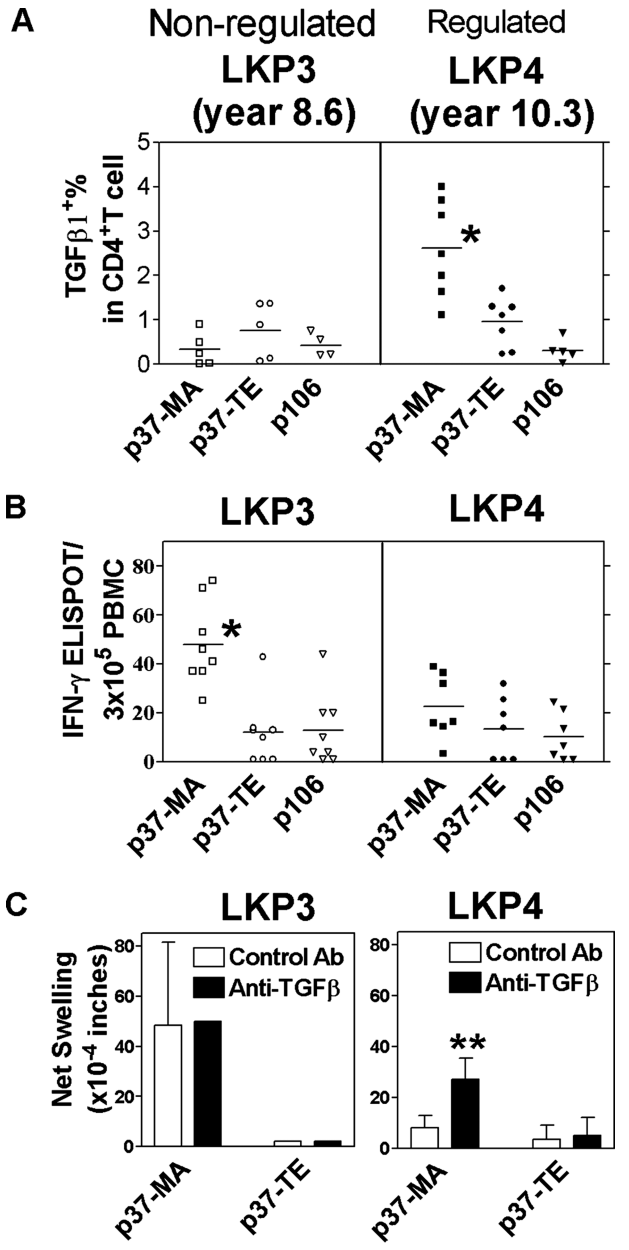


FIGURE 5. Levels of inducible CD4$^+$TGF-β1$^+$ cells are inversely related to IFN-γ ELISPOT and DTH responses. K1 PBMC from a nonregulated and a regulated time point were compared. *A*, Dot plot showing percentages of CD4$^+$ T cells with TGF-β1$^+$ surface expression in cultured LKP3 and LKP4 PBMC, corrected for background (1.0 $\pm$ 0.3% for LKP3 and 1.8 $\pm$ 1% for LKP4, cultures with medium alone). *B*, Numbers of IFN-γ secreting cells, shown as spots per 3×10^5 PBMC in ELISPOT cultures. *, $p < 0.01$, comparing mean response (horizontal line) to p37-MA vs other peptides; Each symbol represents a separate determination. *C*, Trans-vivo DTH responses in the presence of isotype control or TG/Fβ1-specific Ab. **, $p < 0.001$ vs control Ab.

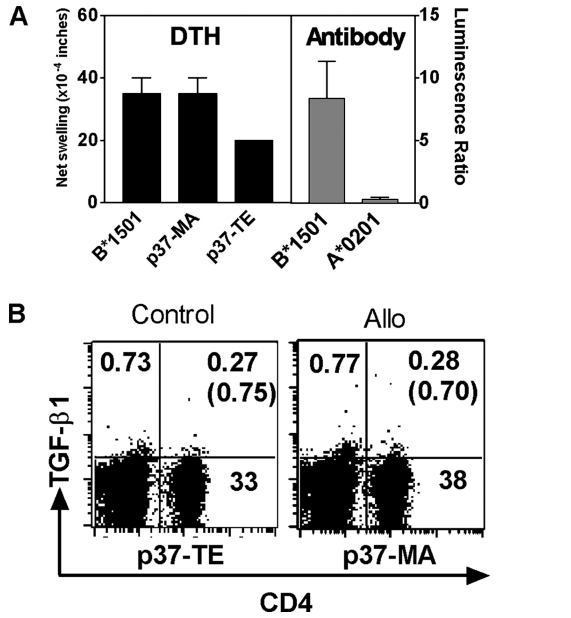


FIGURE 6. Lack of HLA-B allopeptide-specific T_R cells in a HLA-B –sensitized renal transplant patient. PBMC at 1 year and serum samples obtained at 0.5–1.5 year posttransplant from patient K3 were tested for DTH and anti-HLA Ab. *A*, Cellular and humoral immune responses to HLA-B*1501 Ag; DTH responses to p37-MA or p37-TE are also shown. Data are the mean $\pm$ SD of two determinations for DTH measured in units of 10^{-4} inches net footpad swelling and three determinations of Ab responses measured by the ratio of the median bead luminescence values to the positive cut-off values. Self-Ag HLA-A*0201-coated beads were used as a negative control ($p < 0.05$; $n = 3$). *B*, Flow cytometry analysis of PBMC cultured with peptide p37-TE (*left panel*) or p37-MA (*right panel*). CD4$^+$TGF-β1$^+$ cells as a percentage of gated lymphocytes are indicated in the *upper right quadrant*. The numbers in parentheses are the percentages of CD4 T cells. Data are representative of two separate experiments. Allo, allopeptide.

flow cytometry using a chicken anti-TGF-β1 Ab that recognizes active as well as high m.w. TGF-β1-associated complexes in Western blots (data not shown). In a representative experiment shown in Fig. 4*A*, peptide p37-MA induced surface TGF-β1 expression in 4.44% of the CD4$^+$ T cells of K1, ~2.5-fold higher than that in CD4$^+$ T cells stimulated with the control self-peptide. Background staining with the isotype control Ab was <0.25%. Similarly, in vitro cultures of patient K2 PBMC with the donor HLA-B8-derived allopeptide p61-F induced the expression of surface TGF-β1 in some CD4$^+$ T cells (Fig. 4*A*). The TGF-β1 response was dose dependent; the highest peptide dose tested (2 mg/ml) induced a 2-fold higher mean percentage of TGF-β1$^+$ CD4 T cells as compared with the control self-peptide p61-C ($p < 0.01$; Fig. 4*B*). A similar induction of surface TGF-β1 in the CD4 T cells of patient K2 was observed after stimulation with peptide p37-MA (data not shown). Both "background" surface TGF-β1 induction by a self-peptide and allopeptide-inducible TGF-β1 expression were 3- to 10-fold lower in the CD4$^+$ T cells of patient K2 as compared with those of patient K1.

To determine the CD25 phenotype of the CD4$^+$ T cells induced to express surface TGF-β1, cultured PBMC were analyzed by flow cytometry for surface TGF-β1 and CD25 expression. In both patients, the CD25^{low} fraction of CD4$^+$ T cells was enriched for TGF-β1$^+$ surface expression relative to the CD25^{high} or CD25$^-$ subsets (Fig. 4*C*).

Nonregulated and regulated PBMC samples contain different proportions of IFN-γ- vs TGF-β1-inducible T cells

Although the mean fluorescence intensity of the cell surface staining for TGF-β1 was always low, the pattern of a higher percentage of surface TGF-β1-expressing CD4 T cells induced by p37-MA vs p37-TE was consistent in seven experiments with K1 LKP4 (Fig. 5*A*). In contrast, when LKP3 PBMC from the same patient were cocultured with the p37-MA peptide, few (<1%) surface TGF-β1$^+$ cells were found in the CD4$^+$ T cell subset (Fig. 5*A*, *left*

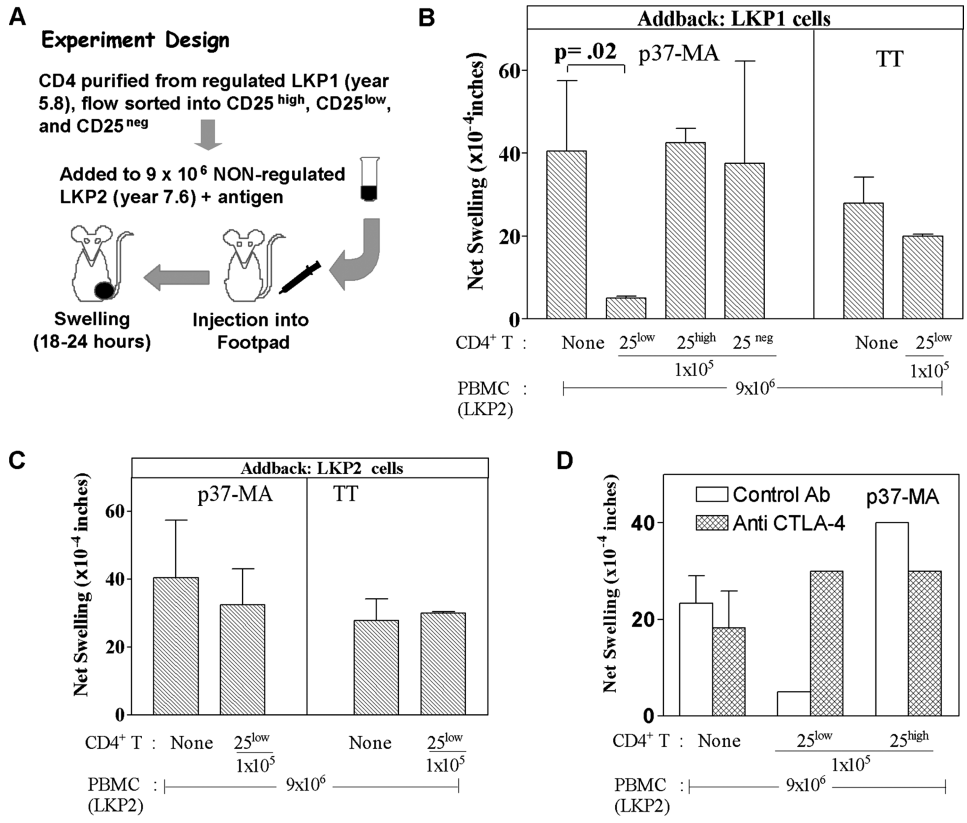


FIGURE 7. CD25^{low} but not CD25^{high} CD4$^+$ T cells adoptively transfer a p37-MA-specific suppressed DTH response to "nonregulated" PBMC. *A*, Diagram showing experimental design. *B*, Trans-vivo DTH responses of PBMC from LKP2 to p37-MA (*left panel*) or TT (*right panel*) in the presence of added medium alone (none) or 1×10^5 sorted cells of each CD4$^+$ T subset from LKP1. *C*, DTH responses of LKP2 PBMC to p37-MA peptide (*left panel*) or TT (*right panel*) in the presence of sorted CD4$^+$CD25^{low} T cells from the same PBMC sample. *D*, Anti-p37-MA DTH response of LKP2 cells after the addition of medium alone (None) or flow-sorted CD4$^+$ T cells from LKP1 tested in the presence of control (open bars) or anti-CTLA-4 Ab (crosshatched bars). Data shown are the mean ± SD of 2–10 experiments.

panel). The reverse of this pattern was seen when allopeptide-specific Th-1 (T_E) cells were analyzed using a IFN-γ ELISPOT assay. As shown in Fig. 5*B*, LKP3 cells made a IFN-γ response to p37-MA but not to the self-peptide p37-TE or to the irrelevant B*1501 peptide p106. The IFN-γ response to p37-MA by LKP4 cells, in contrast, was significantly less than that of LKP3, consistent with the DTH assay results (compare Fig. 5, *B* and *C*). Neutralizing TGF-β1 did not reveal any additional footpad swelling in LKP3 to p37-MA, but the same treatment of LKP4 cells revealed a moderate response. DTH responses to the control peptide, p37-TE, were negative with or without anti- Ab (Fig. 5*C*).

*Absence of TGF-β1-inducible CD4 adaptive T_R cells in a case of B*1501 allosensitization*

The above results imply that the absence of TGF-β1-inducible adaptive T_R cells can be a marker of allosensitization at the T cell level. To determine whether allosensitization at the B cell level also correlates with an absence of TGF-β1-inducible adaptive T_R cells, we examined PBMC from K3, a HLA-DR4$^+$ patient who received a HLA B62-mismatched renal transplant from a HLA haplotype-matched living donor along with Campath-1H (anti-CD52) induction therapy. This patient is being maintained on rapamycin monotherapy as part of an Immune Tolerance Network-sponsored tolerance trial and retains normal graft function. However, he is not currently a candidate for complete weaning off of immunosuppression due to Ab formation and C4d deposits in his kidney transplant. PBMC obtained at 1 year posttransplant from K3 responded strongly in a trans-vivo DTH assay to donor-type alloantigen HLA-B*1501 and to allopeptide p37-MA, but only weakly to control peptide p37-TE (Fig. 6*A*). A specific Ab to HLA- B*1501, but not to self Ag HLA-A*0201, was found in his serum by indirect luminescence assay (Fig. 6*A*). As expected, no linked suppression of recall DTH was detected in the presence of HLA- B*1501 (data not shown). When the PBMC of patient K3 were cultured with HLA-B derived peptides, there was no specific induction of surface TGF-β1 in response to p37-MA compared with p37-TE (Fig. 6*B*). These data are similar to the findings in LKP3 from patient K1, except that patient K3 developed a HLA-B*1501-specific anti-donor Ab, whereas patient K1 did not.

CD4$^+$CD25^{low} T cells transfer allopeptide-specific DTH regulation

We took advantage of the availability of nonregulated and regulated PBMC samples from the same patient (K1) to determine which CD4$^+$ T cell subset could transfer allopeptide-specific suppression. CD4$^+$ T cells from the first leukapheresis of patient K1 (LKP1, year 5.8) were flow-sorted into CD25 high, low, and negative subsets using the same gating strategy described in Fig. 4*C*. As illustrated diagrammatically in Fig. 7*A*, 1×10^5 sorted cells were mixed with 9×10^6 LKP2 (year 7.6) PBMC and allopeptide p37-MA and injected into a SCID mouse footpad. Consistent with the pattern of induced surface TGF-β1 expression noted above, CD4$^+$CD25^{low}, but not CD4$^+$CD25$^-$ or CD4$^+$CD25^{high} T cells were able to significantly suppress the DTH response to p37-MA (Fig. 7*B*). Surprisingly, CD4$^+$CD25^{high} T cells failed to suppress DTH even when added at a 3-fold higher cell dose, whereas significant DTH inhibition was obtained with as few as 5×10^4 CD4$^+$CD25^{low} T cells (data not shown). The anti-TT DTH response of LKP2 was only slightly reduced (p = NS) by the addition of CD4$^+$CD25^{low} T cells, confirming that the DTH inhibition effect required the presence of donor alloantigen. As a control for the isolation procedure itself, CD4$^+$CD25^{low} T cells isolated from year 7.6 PBMC (LKP2), when added to whole LKP2 cells plus p37-MA, failed to suppress the DTH response (Fig. 7*C*). The addition of a CTLA-4 blocking Ab also had no effect on the DTH response of LKP2 cells to p37-MA but completely reversed the inhibition of DTH by CD4$^+$CD25^{low} T cells from LKP1 (Fig. 7*D*).

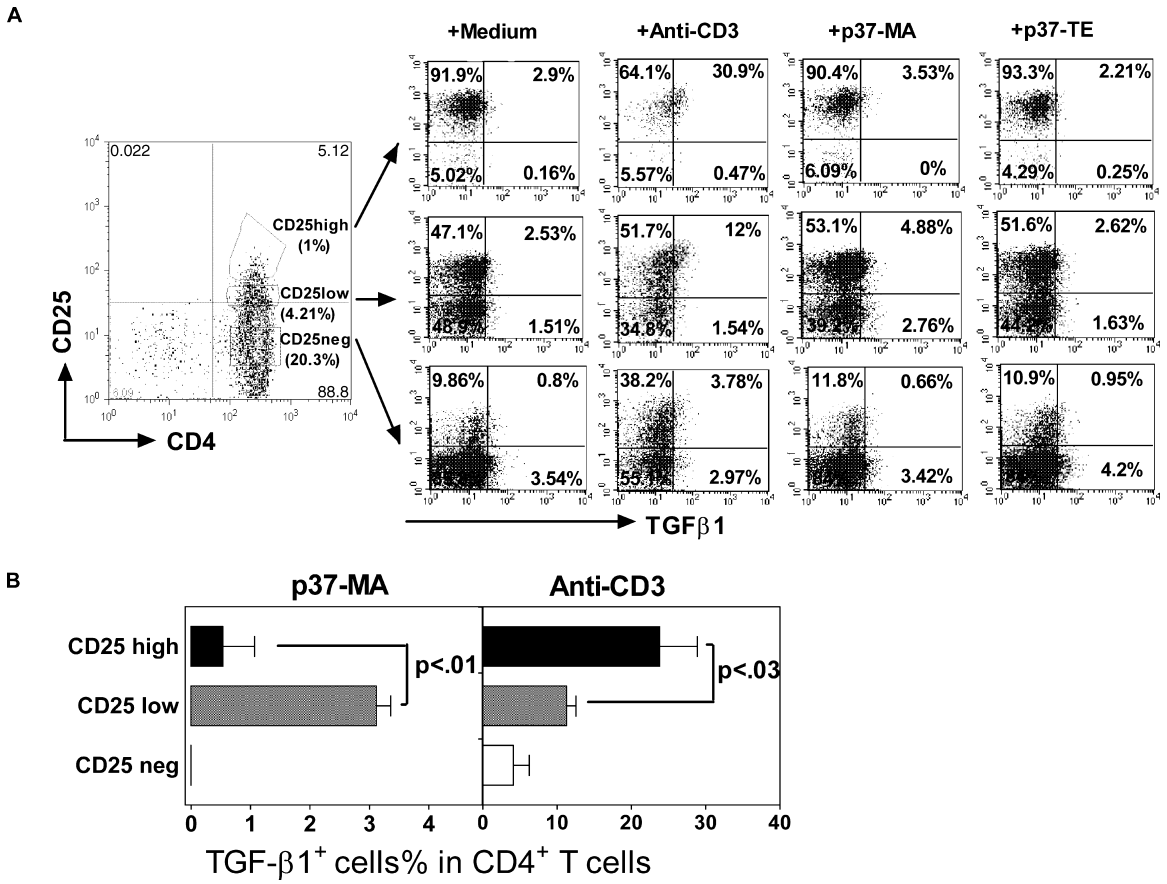


FIGURE 8. Surface TGF-β1 expression and stability of CD25 phenotype after culture of flow-sorted T cells. *A*, Flow histograms of $CD25^{high}$, $CD25^{low}$, and $CD25^{-}$ (CD25neg) cells that were sorted from MACS-enriched $CD4^{+}$ T cells from LKP4 of patient K1 (*left*, blue) and cultured for 40 h with γ-irradiated non-CD4 T cells. IL2 (20 U/ml) and either medium alone, anti-CD3 Ab, or HLA-B peptide were added. Data shown in red are gated $CD4^{+}$ T cell events stained for CD25 and TGF-β1 and are representative of 2–4 experiments. *B*, Summary of culture experiments comparing surface TGF-$\beta1^{+}$ cell induction in each $CD4^{+}$ T cell fraction. Individual values (percentage of TGF-$\beta1^{+}$ cells) were corrected for the response to self-peptide p37-TE (mean ± SD, for $CD25^{-}$ = 1.35 ± 0.76%, $CD25^{low}$ = 4.3 ± 3%, $CD25^{high}$ = 7.3 ± 7%). Wilcoxon *p* values for comparison of the $CD25^{low}$ vs $CD25^{high}$ cell cultures are shown for four experiments.

$CD4^{+}CD25^{low}$ T cells show variable CD25 expression but retain allopeptide-specific TGF-β1 responsiveness after flow sorting and short-term culture

The adoptive transfer data, coupled with the finding that mainly $CD25^{low}$ T cells were induced to express surface by allopeptide stimulation in vitro (Fig. 4*C*), raised the possibility that adaptive T_R cells are among the $CD4^{+}$TGF-$\beta1^{+}$ T cells in the graft that showed variable CD25 expression by immunostaining. To examine the question of CD25 expression after exposure to Ag, $CD25^{high}$, $CD25^{low}$, and $CD25^{-}$ T cells in the $CD4^{+}$ T cell subset were flow-sorted from a regulated blood sample (K1-LKP4). Each fraction was cultured with IL-2 and autologous APC feeder cells along with either peptide or anti-CD3 mAb. As shown in Fig. 8*A*, *upper panels*, the $CD25^{high}$ T cells retained stable CD25 expression in culture, and polyclonal stimulation by anti-CD3 and IL-2 induced surface TGF-β1 expression in a significant proportion of the T cells. However, there was relatively little induction of surface TGF-β1 expression in response to p37-MA relative to medium or p37-TE controls. Flow-sorted $CD4^{+}CD25^{-}$ T cells were activated by anti-CD3 to express varying levels of CD25 and a low level of surface TGF-β1 expression. However, in cultures with medium alone or peptides, >85% retained negative for CD25 and there was no induction of surface TGF-β1 expression by p37-MA relative to p37-TE.

Isolated $CD4^{+}CD25^{low}$ cells exhibited a unique response pattern during in vitro culture. First, they did not retain a low CD25 expression. Instead, when cultured in the absence of other $CD4^{+}$ T cells they diverged into $CD25^{high}$ and $CD25^{-}$ populations (Fig. 8*A*, *middle panels*; medium control). When stimulated with anti-CD3, the majority of $CD25^{low}$ T cells became $CD25^{high}$ and a portion of the latter expressed surface TGF-β1. Stimulation with p37-MA resulted in an increased percentage of surface TGF-$\beta1^{+}$ cells relative to medium or peptide p37-TE treated cells, but the expression of TGF-β1 was seen both in the cells that became $CD25^{high}$ and in those reverting to a $CD25^{-}$ status (Fig. 8*A*). When the overall percentage of $CD4^{+}$ T cells induced to express TGF-β1 was compared in two separate experiments, the sorted $CD25^{high}$ subset had the highest response to anti-CD3 stimulation while the sorted $CD25^{low}$ subset had the highest response to allopeptide p37 stimulation ($p < 0.01$, $CD25^{low}$ vs the $CD25^{high}$; Fig. 8*B*).

TGF-β1-expressing $CD4^{+}$ T_R cells are FoxP3^{-} and are distributed differently from FoxP3^{+} T_R cells in the kidney allograft

To address the possible relationship between adaptive and $FoxP3^{+}$ T_R in kidney allograft tolerance, we first compared expression of

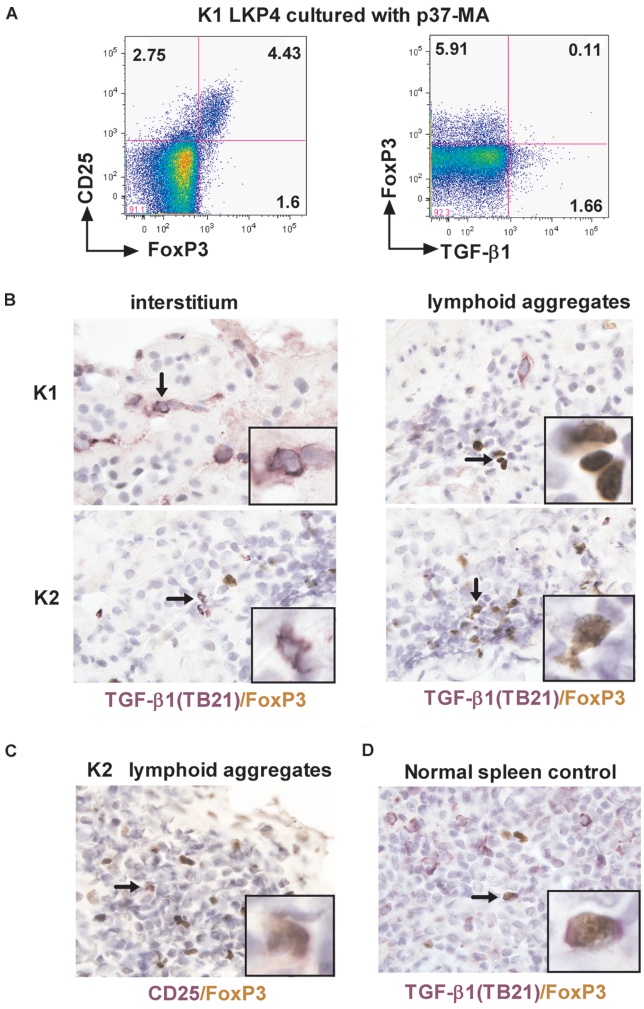


FIGURE 9. Allopeptide-induced TGF-$\beta1^+$ cells in the peripheral blood and TGF-$\beta1^+$ cells in the interstitium of kidney allografts are FoxP3$^-$. *A*, K1 LKP4 were cultured with p37-MA and stained for surface CD25/TGF-β1 and intracellular FoxP3. Cells shown here are gated for CD4$^+$ T cells and are representative of four independent experiments. *B*, Allograft renal biopsies from patients K1 (*top panels*) and K2 (*bottom panels*) were immunolabeled by immunoperoxidase for TGF-β1 (purple) and FoxP3 (brown). TGF-$\beta1^+$FoxP3$^-$ cells were found in the interstitium of both biopsies (*left panels*) whereas TGF-$\beta1^-$FoxP3$^+$ cells were seen primarily in lymphoid aggregates (*right panels*). *Right bottom insets* are the cells indicated by arrow at low power. *C*, Highlights a cell that is double positive for CD25 (purple) and FoxP3 (brown) in the lymphoid aggregate of the kidney biopsy of patient K2. No CD25$^+$FoxP3$^+$ cells were seen in the renal interstitium outside of the lymphoid aggregates. *D*, A splenocyte that is double positive for TGF-β1 (purple) and FoxP3 (brown) in normal human spleen.

FoxP3 and TGF-β1 in cultured PBMC that had been exposed to allopeptide. After a culture of K1 PBMC (LKP4) with p37-MA, CD4$^+$CD25^{high} T cells, as expected, had a uniformly high expression of intracellular FoxP3 protein, while most CD4$^+$CD25^{low} T cells were FoxP3$^-$ (Fig. 9*A*, *left panel*). Furthermore, relatively few surface TGF-$\beta1^+$CD4$^+$ T cells induced by allopeptide coexpressed an intracellular FoxP3 protein (Fig. 9*A*, *right panel*). To explore this question further, we used an immunoperoxidase approach that clearly distinguishes nuclear FoxP3 from surface-bound TGF-β1. As shown in Fig. 9*B*, *left panels*, TGF-$\beta1^+$ cells (purple) were found predominantly in the tubulointerstitium kidney of biopsy samples from K1 (year 10.3) and K2 (year 18). The *inset* in each photomicrograph highlights the cell indicated by arrow on low-power view, showing a distinct rim of surface staining with the mAb TB21 and an absence of nuclear FoxP3 (brown). In contrast, FoxP3$^+$ cells were found in the lymphoid aggregates (Fig. 9*B*, *right panel*); the *inset* shows a dense brown nuclear staining. In the low power view of the K1 biopsy, a single purple (TGF-$\beta1^+$) rim-stained cell in the interstitial area above the lymphoid aggregate provides a sharp contrast to the FoxP3$^+$ cells below (Fig. 9*B*). The lack of dual-stained TGF-$\beta1^+$FoxP3$^+$ cells was not the result of technical problems in immunostaining, because dual-stained TGF-$\beta1^+$FoxP3$^+$ cells were detected in sections of normal human spleen (Fig. 9*D*, *inset*). FoxP3$^+$ cells found in the K2 lymphoid aggregates did costain for surface CD25 (Fig. 9*C*, *inset*), consistent with the stable (high) CD25 expression by FoxP3$^+$ CD4 T cells during short-term culture (Figs. 8*A* and 9*A*).

Discussion

The data suggests that two distinct classes of human CD4$^+$ T regulatory cells participate in tolerance to a kidney transplant. One class consists of Ag-specific, adaptive T_R cells induced by donor HLA-B allopeptides. These T_R cells expressed surface TGF-β1 upon Ag stimulation and circulated in the CD4$^+$CD25^{low} fraction of PBMC. Phenotypically similar (CD4$^+$TGF-$\beta1^+$CD25$^{+/-}$) cells were found in the allograft, mainly localized to the tubulointerstitium, where they have been found previously in rhesus monkey kidney transplants during tolerance (4). As in the monkey model, such CD4$^+$ adaptive T_R cells were absent from the peripheral blood of a patient who failed to become tolerant following leukocyte-depleting Ab therapy, developing instead a strong anti-donor HLA B-specific Ab and DTH response (Fig. 6). The other class consists of CD4$^+$FoxP3$^+$ natural T_R cells, which were found in lymphoid aggregates within the accepted allograft and circulated mainly in the CD4$^+$CD25^{high} fraction of PBMC. In normal subjects, this same fraction has been found to suppress the proliferation of CD4$^+$CD25$^-$ T cells in an Ag nonspecific manner (13). Human CD4$^+$CD25^{high} T cells can also be induced to express surface TGF-β1 in vitro by polyclonal activation with anti-CD3 and IL-2 (Fig. 8) (38). We have recently found that, once activated in this manner, CD4$^+$CD25^{high} T cells but not CD25$^-$ T cells suppress a trans-vivo DTH response by fresh PBMC to a recall Ag in the SCID mouse footpad; this suppression was TGF-β dependent. However, CD4$^+$CD25^{high} T cells did not suppress any DTH response unless activated via anti-CD3 and anti-CD28 (Q. Xu, E. Jankowska-Gan, and W. Burlingham, unpublished observations). The transfer of nonactivated CD4$^+$CD25^{high} T cells could not restore a regulated DTH response to allopeptide in PBMC lacking such regulation. Instead, it was the CD4$^+$CD25^{low} T cells present in regulated PBMC samples that were able to transfer suppression of allopeptide response efficiently and specifically (Fig. 7). These data are consistent with findings in the mouse suggesting that the restoration of specific tolerance to pancreatic islet autoantigens in vivo requires CD4$^+$CD25^{low} as well as CD4$^+$CD25^{high} T_R cells (8) and that dominant tolerance may in some cases suppress the functions (e.g., cytokine production, DTH) but not the expansion of T_E cells (6, 28, 39).

The DTH transfer data using cells collected from patient K1 indicated that only the CD25^{low} fraction of CD4 T cells contained functional allopeptide-specific T_R cells. However, we cannot rule out the possibility that the CD4$^+$FoxP3$^+$CD25^{high} fraction of PBMC might also include some adaptive T_R cells. Indeed, a minor population of CD4$^+$CD25^{high} T cells was induced to express surface TGF-β1 by allopeptide stimulation (Fig. 7*B*). Although in vitro derived human adaptive T_R cells that coexpress FoxP3 and

high levels of CD25 have been reported (15), whether or not FoxP3 expression that has been induced in conventional human CD4 T cells is stable in vivo remains controversial (16). It is noteworthy that FoxP3$^+$ T_R cells tend to be lymph node homing (40). In contrast, surface TGF-β1$^+$FoxP3^{neg} T cells in the renal biopsy samples of patients K1 and K2 were localized to the peritubular interstitium, consistent with a tissue-homing T cell phenotype. The function of lymphoid aggregates commonly observed in accepted kidney transplants has long remained a mystery (for a review, see Ref. 37). The finding that the lymphoid aggregates in the allografts of patients K1 and K2 were enriched in FoxP3$^+$ T_R cells (and recently confirmed in the rhesus monkey kidney transplant tolerance model; J. R. Torrealba, unpublished observations) suggests that the aggregates themselves may be tertiary lymphoid structures that retain natural FoxP3$^+$ T_R cells but allow the adaptive T_R/suppressive cells to pass through to the tubulointerstitium.

Unlike the CD25^{high} FoxP3$^+$ T_R cells, which retained high CD25 expression in vitro (Fig. 8) and in vivo (Fig. 9*C*), CD25^{low}CD4$^+$ T cells appear to be heterogenous. Flow-sorted human CD4$^+$CD25^{low} T cells gave rise to both CD25^{high} and CD25$^-$ T cells when cultured for 36 h.; in the presence of the p37MA allopeptide, the derivative CD25^{high} and CD25$^-$ populations each contained cells that expressed surface TGF-β1 (Fig. 8). Similarly, surface TGF-β1$^+$ T_R cells in the graft were heterogeneous in CD25 expression. Viguier et al. (3) reported that both CD25^{high}FoxP3$^+$ and CD25$^-$FoxP3$^-$ T_R cells were present in metastatic lymph nodes of patients with advanced malignant melanoma; interestingly, the majority of TGF-β1 production came from the latter subset. The relative importance of each class of T_R cells in maintaining tolerance is unclear. It has recently been reported that FoxP3 mRNA is more highly expressed in the urine sediment cells of patients undergoing a reversible, as opposed to irreversible, acute rejection (41). This finding is consistent with our observation of the CD25^{high}FoxP3$^+$ class of T_R cells in biopsy samples from two tolerant patients, one of whom (K1) developed renal allotolerance after the reversal of an acute rejection episode.

The T_R:T_E equilibrium model predicts that the disappearance or elimination of adaptive T_R cells (2, 4) or interference with their function (42) will lead to the re-emergence of T_E response and the breakdown of tolerance. However, unlike a patient who developed anti-donor DTH responsiveness at year 9.0 and rejected his maternal kidney transplant at year 10 (35), and unlike the monkeys that lost their renal allografts to rejection shortly after regaining a strong peripheral anti-donor DTH response (4), patient K1 did not lose his graft after the restoration of anti-donor DTH response at year 7.5 posttransplant. There are several possible explanations for this, none of which fits with a simple T_R:T_E equilibrium model of peripheral tolerance. One explanation is that because the graft donor was closely DR and DQ matched, the B lymphocytes of K1 would be unable to form class II donor-specific Ab even in the presence of adequate T cell help. Indeed, no anti HLA-class I or II Abs were detected, either by sensitive flow-beads or Luminex-based assays, in serum samples collected between year 5 and year 10 posttransplant (J.-H. Lee and W. Burlingham, unpublished observations). However, HLA-class II matching alone is not a satisfactory explanation. Many DR-matched kidney transplants undergo rejection, while some fully DR-mismatched grafts can be accepted (patient K2 being a case in point). Also, patient K3 was humorally sensitized not only to donor HLA-B*1501 (Fig. 6*A*) but also to a donor HLA-DR13 Ag (S. Knechtle, unpublished observations). Although this patient is clearly not tolerant, he continues to have good renal function on rapamycin monotherapy despite anti-HLA Ab formation. A second possible answer is that because patient K1 has a low producer IFN-γ and TNF-α genotype (43), his T_E cells would be susceptible to inhibition even by low levels of TGF-β1 (44). A third possibility is that despite their disappearance from the blood, TGF-β1-inducible CD4$^+$ T_R cells were still able to localize to the allograft while IFN-γ-producing T_E cells could not. We did not risk testing this idea because it would have entailed a biopsy of the kidney and a concomitant risk of infection at a time when systemic adaptive immunity was strongest. Innate immune mechanisms are involved in the mobilization of T_E cells from the blood to the graft that precipitates transplant rejection (45); thus, even when the circulating component of adaptive immunity is unbalanced in favor of T_E cells, allograft rejection may still be prevented in the absence of local secondary signals provided through innate immune pathways.

The adaptive T_R cells identified in this study recognized allopeptide epitopes. The rules that govern this recognition appear to be the same as those involved in determining specificity of conventional T_E cells. Thus, for example, HLA-B*1501-specific CD4$^+$ T_R and T_E cells were present in patients K1 and L1, yet different HLA-DR Ags in patient K1 (DR4, 6) vs L1 (DR15, –) were associated with different patterns of T_R and T_E allopeptide specificity. Surprisingly, p37-MA was not only a dominant allopeptide for patients K1 and K3 but also for K2, even though K2 was mismatched for a different p37-MA-containing HLA-B allele (B*5701 vs B*1501) and expressed different HLA-DR/DQ alleles. The fact that K3, a DR4/DR15 heterozygous patient, responded to p37-MA whereas L1, who was homozygous for DR15, did not suggests that either the DR4 itself or the DR4-linked DQ3 Ag provides an HLA restriction element for indirect pathway recognition of this allopeptide. The class II restriction element for p37-MA in patient K2 is less clear. A degree of promiscuity in peptide binding and recognition was previously suggested for CD4 indirect pathway T cells cloned from a transplant nephrectomy (46), one of which was inducible for surface TGF-β1 and had the functional characteristics of an adaptive T_R cell (47).

The numbers of T_R cells responding to a single allopeptide appeared to be higher in patient K1 (LKP4) than in K2 when calculated by subtraction of the "self" HLA-B peptide-induced background response: 1–3% of CD4$^+$ T cells surface TGF-β1$^+$ in K1 as compared with 0.2–0.4% in K2. When calculated as a multiple of the background response to self-peptide, the relative number of CD4$^+$TGF-β1$^+$ responder cells in both patients fell into the same range: 2–3 times background. T_E cell frequencies to a given allopeptide could be calculated more accurately based on an IFN-γ ELISPOT assay. For example, T_E cells responding to p37-MA in K1 LKP3 cells were ~0.03% of CD4$^+$ T cells (Fig. 4). This number is well within the range of the values obtained by an IFN-γ ELISPOT assay of indirect pathway CD4$^+$ T cells responding to HLA-DR-derived allopeptides in patients with DR-mismatched renal allografts (48).

Our data suggest a key role of CTLA-4 in the function of CD4$^+$ adaptive T_R cells. The reversal by CTLA-4 blocking Abs of DTH suppression in the CD25^{low} cell transfer assay (Fig. 7*D*) suggests that CTLA-4 is critical for interaction of the T_R cell with the APC, as has been previously suggested for the CD4$^+$CD25$^+$ natural T_R (49, 50). In preliminary in vitro studies, we have found that the blockade of CTLA-4 also prevents the induction of surface TGF-β1$^+$ in both polyclonally stimulated natural T_R cells and in adaptive T_R cells responding to donor allopeptide (Q. Xu and W. Burlingham, unpublished observations), suggesting that CTLA-4 is involved in the induction of TGF-β1 as has been previously suggested (51).

In summary, an analysis of two cases of tolerance to HLA-mismatched organ allografts supports the hypothesis that peripheral tolerance involves a balance between CD4$^+$CD25^{low} adaptive

T_R cells and CD4$^+$ T_E cells specific for the same donor-derived class I allopeptides. The adaptive T_R cells identified in this study were distinct in both function and intragraft localization from CD4$^+$ CD25^{high}FoxP3$^+$ T cells. The finding of distinct subsets of CD25^{low}FoxP3$^-$ adaptive T_R cells vs CD25^{high} FoxP3$^+$ T_R cells and the fortuitous observation of a metastable form of human transplant tolerance will need to be confirmed in a larger series of tolerant patients. Coordinated efforts to find and study these rare individuals are currently underway in Europe and North America (52).

Acknowledgments

We thank Kathleen Schell for expert technical assistance in flow analysis and sorting, Daniel Rodriguez for help in DTH analysis, Dr. Jar-How Lee of the One Lambda Company (Canoga Park, CA) for analysis of serum Ab using flow-bead technology, and Glen Leverson for statistical analysis of the data.

Disclosures

The authors have no financial conflict of interest.

References

1. Dittmer, U., H. He, R. J. Messer, S. Schimmer, A. R. Olbrich, C. Ohlen, P. D. Greenberg, I. M. Stromnes, M. Iwashiro, S. Sakaguchi, et al. 2004. Functional impairment of CD8$^+$ T cells by regulatory T cells during persistent retroviral infection. *Immunity* 20: 293–303.
2. Belkaid, Y., C. A. Piccirillo, S. Mendez, E. M. Shevach, and D. L. Sacks. 2002. CD4$^+$CD25$^+$ regulatory T cells control *Leishmania major* persistence and immunity. *Nature* 420: 502–507.
3. Viguier, M., F. Lemaitre, O. Verola, M. S. Cho, G. Gorochov, L. Dubertret, H. Bachelez, P. Kourilsky, and L. Ferradini. 2004. Foxp3 expressing CD4$^+$ CD25^{high} regulatory T cells are overrepresented in human metastatic melanoma lymph nodes and inhibit the function of infiltrating T cells. *J. Immunol.* 173: 1444–1453.
4. Torrealba, J. R., M. Katayama, J. H. Fechner, Jr., E. Jankowska-Gan, S. Kusaka, Q. Xu, J. M. Schultz, T. D. Oberley, H. Hu, M. M. Hamawy, et al. 2004. Metastable tolerance to rhesus monkey renal transplants is correlated with allograft TGF–β 1$^+$CD4$^+$ T regulatory cell infiltrates. *J. Immunol.* 172: 5753–5764.
5. Hara, M., C. I. Kingsley, M. Niimi, S. Read, S. E. Turvey, A. R. Bushell, P. J. Morris, F. Powrie, and K. J. Wood. 2001. IL-10 is required for regulatory T cells to mediate tolerance to alloantigens in vivo. *J. Immunol.* 166: 3789–3796.
6. Lin, C. Y., L. Graca, S. P. Cobbold, and H. Waldmann. 2002. Dominant transplantation tolerance impairs CD8$^+$ T cell function but not expansion. *Nat. Immunol.* 3: 1208–1213.
7. Fuss, I. J., M. Boirivant, B. Lacy, and W. Strober. 2002. The interrelated roles of TGF–β and IL-10 in the regulation of experimental colitis. *J. Immunol.* 168: 900–908.
8. Belghith, M., J. A. Bluestone, S. Barriot, J. Megret, J. F. Bach, and L. Chatenoud. 2003. TGF–β-dependent mechanisms mediate restoration of self-tolerance induced by antibodies to CD3 in overt autoimmune diabetes. *Nat. Med.* 9: 1202–1208.
9. Herold, K. C., S. E. Gitelman, U. Masharani, W. Hagopian, B. Bisikirska, D. Donaldson, K. Rother, B. Diamond, D. M. Harlan, and J. A. Bluestone. 2005. A single course of anti-CD3 monoclonal antibody hOKT3γ1(Ala-Ala) results in improvement in C-peptide responses and clinical parameters for at least 2 years after onset of type 1 diabetes. *Diabetes* 54: 1763–1769.
10. Fontenot, J. D., M. A. Gavin, and A. Y. Rudensky. 2003. Apr. Foxp3 programs the development and function of CD4$^+$CD25$^+$ regulatory T cells. *Nat. Immunol.* 4: 330–336.
11. Hori, S., T. Nomura, and S. Sakaguchi. 2003. Control of regulatory T cell development by the transcription factor Foxp3. *Science* 299: 1057–1061.
12. Bluestone, J. A., and A. K. Abbas. 2003. Natural versus adaptive regulatory T cells. *Nat. Rev. Immunol.* 3: 253–257.
13. Baecher-Allan, C., V. Viglietta, and D. A. Hafler. 2002. Inhibition of human CD4$^+$CD25^{+high} regulatory T cell function. *J. Immunol.* 169: 6210–6217.
14. Jonuleit, H., E. Schmitt, H. Kakirman, M. Stassen, J. Knop, and A. H. Enk. 2002. Infectious tolerance: human CD25$^+$ regulatory T cells convey suppressor activity to conventional CD4$^+$ T helper cells. *J. Exp. Med.* 196: 255–260.
15. Walker, M. R., B. D. Carson, G. T. Nepom, S. F. Ziegler, and J. H. Buckner. 2005. De novo generation of antigen-specific CD4$^+$CD25$^+$ regulatory T cells from human CD4$^+$CD25$^-$ cells. *Proc. Natl. Acad. Sci. USA* 102: 4103–4108.
16. Gavin, M. A., T. R. Torgerson, E. Houston, P. Deroos, W. Y. Ho, A. Stray-Pedersen, E. L. Ocheltree, P. D. Greenberg, H. D. Ochs, and A. Y. Rudensky. 2006. Single-cell analysis of normal and FOXP3-mutant human T cells: FOXP3 expression without regulatory T cell development. *Proc. Natl. Acad. Sci. USA* 103: 6659–6664.
17. Lafferty, K. J., S. K. Babcock, and R. G. Gill. 1986. Prevention of rejection by treatment of the graft: an overview. *Prog. Clin. Biol. Res.* 224: 87–117.
18. Billingham, R. E., L. Brent, and P. B. Medawar. 1953. Actively acquired tolerance of foreign cells. *Nature* 172: 603–608.
19. Graca, L., A. Le Moine, C. Y. Lin, P. J. Fairchild, S. P. Cobbold, and H. Waldmann. 2004. Donor-specific transplantation tolerance: the paradoxical behavior of CD4$^+$ CD25$^+$ T cells. *Proc. Natl. Acad. Sci. USA* 101: 10122–10126.
20. Cai, J., J. Lee, E. Jankowska-Gan, R. Derks, J. Pool, T. Mutis, E. Goulmy, and W. J. Burlingham. 2004. Minor H antigen HA-1-specific regulator and effector CD8$^+$ T cells, and HA-1 microchimerism, in allograft tolerance. *J. Exp. Med.* 199: 1017–1023.
21. Garba, M. L., C. D. Pilcher, A. L. Bingham, J. Eron, and J. A. Frelinger. 2002. HIV antigens can induce TGF–β(1)-producing immunoregulatory CD8$^+$ T cells. *J. Immunol.* 168: 2247–2254.
22. Maile, R., S. M. Pop, R. Tisch, E. J. Collins, B. A. Cairns, and J. A. Frelinger. 2006. Low-avidity CD8^{low} T cells induced by incomplete antigen stimulation in vivo regulate naive higher avidity CD8^{high} T cell responses to the same antigen. *Eur. J. Immunol.* 36: 397–410.
23. Nakamura, T., K. H. Sonoda, D. E. Faunce, J. Gumperz, T. Yamamura, S. Miyake, and J. Stein-Streilein. 2003. CD4$^+$ NKT cells, but not conventional CD4$^+$ T cells, are required to generate efferent CD8$^+$ T regulatory cells following antigen inoculation in an immune-privileged site. *J. Immunol.* 171: 1266–1271.
24. Streilein, J. W. 2003. Ocular immune privilege: therapeutic opportunities from an experiment of nature. *Nat. Rev. Immunol* 3: 879–889.
25. VanBuskirk, A. M., W. J. Burlingham, E. Jankowska-Gan, T. Chin, S. Kusaka, F. Geissler, R. P. Pelletier, and C. G. Orosz. 2000. Human allograft acceptance is associated with immune regulation. *J. Clin. Invest.* 106: 145–155.
26. Burlingham, W. J., and J. Torrealba. 2004. Immunologic tolerance as taught by allografts. In *Immunobiology of Organ Transplantation.* D. Wilkes, and W. Burlingham, eds. Plenum/Kluwer Press, New York, pp. 365–383.
27. Carrodeguas, L., C. G. Orosz, W. J. Waldman, D. D. Sedmak, P. W. Adams, and A. M. VanBuskirk. 1999. Trans vivo analysis of human delayed-type hypersensitivity reactivity. *Hum. Immunol.* 60: 640–651.
28. Geissler, F., E. Jankowska-Gan, L. D. DeVito-Haynes, T. Rhein, M. Kalayoglu, H. W. Sollinger, and W. J. Burlingham. 2001. Human liver allograft acceptance and the 'tolerance assay': in vitro anti-donor T cell assays show hyporeactivity to donor cells but, unlike DTH, fail to detect linked suppression. *Transplantation* 72: 571–580.
29. Jankowska-Gan, E., T. Rhein, L. Haynes, F. Geissler, A. Mulder, M. Kalayoglu, H. Sollinger, and W. Burlingham. 2002. Human liver allograft acceptance and the 'tolerance assay', II: donor HLA-A, -B but not DR antigens are able to trigger regulation of DTH. *Hum. Immunol.* 63: 862.
30. Ulmer, A. J., and H. D. Flad. 1979. Discontinous density gradient seperation of human mononuclear leukocytes using Percoll as a gradient medium. *J. Immunol. Methods* 30: 1–10.
31. Ott, P. A., B. R. Berner, B. A. Herzog, R. Guerkov, N. L. Yonkers, I. Durinovic-Bello, M. Tary-Lehmann, P. V. Lehmann, and D. D. Anthony. 2004. CD28 costimulation enhances the sensitivity of the ELISPOT assay for detection of antigen-specific memory effector CD4 and CD8 cell populations in human diseases. *J. Immunol. Methods* 285: 223–235.
32. Solez, K. 1994. International standardization of criteria for histologic diagnosis of chronic rejection in renal allografts. *Clin. Transplant.* 8: 345–350.
33. Taylor, C. R., S. R. Shi, C. Chen, L. Young, C. Yang, and R. J. Cote. 1996. Comparative study of antigen retrieval heating methods: microwave, microwave and pressure cooker, autoclave, and steamer. *Biotech. Histochem.* 71: 263–270.
34. Kusaka, S., A. P. Grailer, J. H. Fechner, Jr., E. Jankowska-Gan, T. Oberley, H. W. Sollinger, and W. J. Burlingham. 2000. Clonotype analysis of human alloreactive T cells: a novel approach to studying peripheral tolerance in transplant recipients. *J. Immunol.* 164: 2240–2247.
35. Burlingham, W. J., E. Jankowska-Gan, A. M. VanBuskirk, C. G. Orosz, J. H. Lee, and S. Kusaka. 2000. Loss of tolerance to a maternal kidney transplant is selective for HLA class II: evidence from trans-vivo DTH and alloantibody analysis. *Hum. Immunol.* 61: 1395–1402.
36. Preston, E. H., H. Xu, K. K. Dhanireddy, J. P. Pearl, F. V. Leopardi, M. F. Starost, D. A. Hale, and A. D. Kirk. 2005. IDEC-131 (anti-CD154), sirolimus and donor-specific transfusion facilitate operational tolerance in non-human primates. *Am. J. Transplant.* 5: 1032–1041.
37. Burlingham, W., S. Kusaka, L. T. Chin, D. Hullett, S. J. Knechtle, H. Sollinger, T. Oberley, J. Pirsch, A. D. Kirk, and B. N. Becker. 1999. Focal infiltrates in kidney allografts — developing a model for clinical transplant peripheral tolerance. *Graft* 2: 253–260.
38. Nakamura, K., A. Kitani, I. Fuss, A. Pedersen, N. Harada, H. Nawata, and W. Strober. 2004. TGF–β 1 plays an important role in the mechanism of CD4$^+$ CD25$^+$ regulatory T cell activity in both humans and mice. *J. Immunol.* 172: 834–842.
39. Tang, Q., J. Y. Adams, A. J. Tooley, M. Bi, B. T. Fife, P. Serra, P. Santamaria, R. M. Locksley, M. F. Krummel, and J. A. Bluestone. 2006. Visualizing regulatory T cell control of autoimmune responses in nonobese diabetic mice. *Nat. Immunol.* 7: 83–92.
40. Ochando, J. C., A. C. Yopp, Y. Yang, A. Garin, Y. Li, P. Boros, J. Llodra, Y. Ding, S. A. Lira, N. R. Krieger, and J. S. Bromberg. 2005. Lymph node occupancy is required for the peripheral development of alloantigen-specific Foxp3$^+$ regulatory T cells. *J. Immunol.* 174: 6993–7005.
41. Muthukumar, T., D. Dadhania, R. Ding, C. Snopkowski, R. Naqvi, J. B. Lee, C. Hartono, B. Li, V. K. Sharma, S. V. Seshan, et al. 2005. Messenger RNA for

FOXP3 in the urine of renal-allograft recipients. *N. Engl. J. Med.* 353: 2342–2351.
42. Peng, G., Z. Guo, Y. Kiniwa, K. S. Voo, W. Peng, T. Fu, D. Y. Wang, Y. Li, H. Y. Wang, and R. F. Wang. 2005. Toll-like receptor 8-mediated reversal of $CD4^+$ regulatory T cell function. *Science* 309: 1380–1384.
43. Burlingham, W. J., P. J. O'Connell, L. M. Jacobson, B. N. Becker, A. D. Kirk, V. Pravica, and I. V. Hutchinson. 2000. Tumor necrosis factor-α and tumor growth factor-β1 genotype: partial association with intragraft gene expression in two cases of long-term peripheral tolerance to a kidney transplant. *Transplantation* 69: 1527–1530.
44. Dierksheide, J. E., R. A. Baiocchi, A. K. Ferketich, S. Roychowdhury, R. P. Pelletier, C. F. Eisenbeis, M. A. Caligiuri, and A. M. VanBuskirk. 2005. IFN-γ gene polymorphisms associate with development of EBV^+ lymphoproliferative disease in hu PBL-SCID mice. *Blood* 105: 1558–1565.
45. Land, W. G. 2005. The role of postischemic reperfusion injury and other nonantigen-dependent inflammatory pathways in transplantation. *Transplantation* 79: 505–514.
46. Frasca, L., A. Amendola, P. Hornick, P. Brookes, G. Aichinger, F. Marelli-Berg, R. I. Lechler, and G. Lombardi. 1998. Role of donor and recipient antigen-presenting cells in priming and maintaining T cells with indirect allospecificity. *Transplantation* 66: 1238–1243.
47. Roelen, D., S. van Bree, P. van Hulst, E. van Beelen, and F. Claas. 2002. Regulatory functions of human $CD4^+$ T cells recognizing allopeptides in the context of self-HLA class II. *Hum. Immunol.* 63: 902.
48. Poggio, E. D., M. Clemente, J. Riley, M. Roddy, N. S. Greenspan, C. Dejelo, N. Najafian, M. H. Sayegh, D. E. Hricik, and P. S. Heeger. 2004. Alloreactivity in renal transplant recipients with and without chronic allograft nephropathy. *J. Am. Soc. Nephrol.* 15: 1952–1960.
49. Takahashi, T., T. Tagami, S. Yamazaki, T. Uede, J. Shimizu, N. Sakaguchi, T. W. Mak, and S. Sakaguchi. 2000. Immunologic self-tolerance maintained by $CD25^+CD4^+$ regulatory T cells constitutively expressing cytotoxic T lymphocyte-associated antigen 4. *J. Exp. Med.* 192: 303–310.
50. Read, S., V. Malmstrom, and F. Powrie. 2000. Cytotoxic T lymphocyte-associated antigen 4 plays an essential role in the function of $CD25^+CD4^+$ regulatory cells that control intestinal inflammation. *J. Exp. Med.* 192: 295–302.
51. Chen, W., W. Jin, and S. M. Wahl. 1998. Engagement of cytotoxic T lymphocyte-associated antigen 4 (CTLA-4) induces transforming growth factor β (TGF–β) production by murine $CD4^+$ T cells. *J. Exp. Med.* 188: 1849–1857.
52. Newell, K. A., C. P. Larsen, and A. D. Kirk. 2006. Transplant tolerance: converging on a moving target. *Transplantation* 81: 1–6.